Shape-Controlled Synthesis of Poly(styrene sulfonate) and Poly(vinyl pyrolidone) Capped Lead Sulfide Nanocubes, Bars, and Threads

ARTICLE *in* THE JOURNAL OF PHYSICAL CHEMISTRY C · APRIL 2008

Impact Factor: 4.77 · DOI: 10.1021/jp711925b

4 AUTHORS, INCLUDING:

Mandeep Singh
Davangere University
207 PUBLICATIONS **5,594** CITATIONS

SEE PROFILE

Nils O Petersen
University of Alberta
132 PUBLICATIONS **4,142** CITATIONS

SEE PROFILE

Shape-Controlled Synthesis of Poly(styrene sulfonate) and Poly(vinyl pyrolidone) Capped Lead Sulfide Nanocubes, Bars, and Threads

Mandeep Singh Bakshi,*,†,‡ Gurinder Kaur,§ Fred Possmayer,|| and Nils O. Petersen*,†,⊥

Department of Chemistry and Department of Biochemistry, University of Western Ontario, 339 Windermere Road, London, Ontario N6A 5A5, Canada, National Institute for Nanotechnology, Edmonton, Alberta, Canada, Department of Physics, College of North Atlantic, Labrador City, Newfoundland A2V 2K7, Canada, and Department of Chemistry, Guru Nanak Dev University, Amritsar 143005, Punjab, India

Received: December 20, 2007; In Final Form: January 19, 2008

Lead sulfide nanocrystals (NCs) along with nanothreads and nanosheets were synthesized in the presence of water soluble polymers such as poly(styrene sulfonate) sodium salt (PSS) and poly(vinyl pyrolidone) (PVP) in aqueous phases at relatively mild temperature of 80 °C. The amount of each polyelectrolyte was systematically varied between 1 and 4 mM (monomolar based). The presence of PSS produced roughly cubic geometries at low concentrations, while nanothreads and nanosheets were produced at high concentrations. This was not so in the presence of equivalent amounts of PVP, where only fine cubes and nanobars were obtained. The shape and structure of all kinds of geometries were characterized by TEM, FESEM, EDX, and XRD analyses. All results demonstrated that the different preferential adsorption of polyelectrolyte PSS and neutral PVP for different crystal planes of the fcc geometry of PbS controlled the final morphology.

Introduction

Semiconductor nanocrystals (NCs) are very important materials for the fabrication of nanobuilding blocks for nanodevices.[1] Many studies have been devoted to this research, and shape-controlled PbS NCs have been synthesized successfully.[2] Among these shapes, stars, cubes, spheres, and other geometries are well-known,[2c,h] while one-dimensional (1-D) nanowires or nanothreads are still quite rare.[2a,e] The latter geometries are even more important as far as the fabrication of future nanodevices, sensors,[3a] photodectors, and solar cells[3b,c] is concerned. The synthesis of 1-D nanostructures poses a great challenge to obtain cost-effective desired properties, so as to use them for various commercial applications. Many synthetic routes such as hydrothermal,[2a,c] hard template,[2e] and soft template[4] have been applied to synthesize 1-D nanostructures.[5] We herein report a simple synthesis of 1-D nanothreads of PbS along with nanocubes and nanobars in the presence of poly(styrene sulfonate) (PSS) and poly(vinyl pyrolidone) (PVP) in aqueous phases at relatively mild temperature of 80 °C.

PSS is a polyelectrolyte that when dissolved in water produces polyanions with a strong ability to interact with electropositive active sites. Recently, many studies[6] have demonstrated the formation of thin polyelectrolyte multilayer film capped nanoparticles (NPs) including PbS NCs. Just like those of surfactants, polyelectrolyte films provide charge and steric stabilization[7] to the colloidal particles and thereby reduce the possibility of coagulation effects. On the other hand, PVP already has been proven to be a strong stabilizing agent as well as a soft template for the synthesis of silver[8a,e] (Ag) and PbS[2c] NCs in different hydrothermal methods. PVP macromolecules show a stronger preference for the {100} than {111} planes of Ag, thus producing Ag nanowires bound with {100} facets.[8b] A similar mechanism was thought to occur in the case of PbS NCs synthesized in the presence of PVP. We herein compare the capping ability of PSS and PVP on the synthesis of shape-controlled PbS NCs and observe a marked difference between the PbS geometries as well as the mechanisms involved in the presence of both polymers. The use of PSS produced long threads apart from distorted cubes, while only fine cubes and bars were obtained in the presence of PVP. This was discussed on the basis of a difference in the capping behavior of PSS and PVP due to their differences in the electrostatic interactions that seem to play a predominant role in shape-controlled effects.

Experimental Procedures

Materials. PSS and PVP (Scheme 1, Supporting Information) with average molecular weights of 44 000 and 75 000, respectively, were obtained from Lancaster and used as received. Lead acetate, thioacetamide, and acetic acid were purchased from Aldrich. Water was used for purification through double distillation.

Preparation of PbS Nanoparticles. In a typical procedure,[2h] 30 mL of aqueous PSS/PVP (0.5 mM monomolar basis) was placed in a round-bottomed glass flask. Under constant stirring, 4 mL of 1 M aqueous acetic acid was added. This was followed by the addition of 2 mL of 0.5 M aqueous lead acetate and 2 mL of aqueous 0.5 M thioacetamide. After mixing all the components at room temperature, the reaction mixture was kept in an oil bath at a temperature of 80 °C for 48 h under static conditions. No precipitation of the polymer was observed in the presence of lead acetate due to salting out effects. Within a few hours, a black colloidal solution was obtained, indicating the formation of PbS NCs. The colloidal suspension of PbS was collected and washed twice with water followed by several

* Corresponding authors. E-mail: (M.S.B.) ms_bakshi@yahoo.com and (N.O.P.) Nils.Petersen@nrc-cnrc.gc.ca.
† Department of Chemistry, University of Western Ontario.
‡ Guru Nanak Dev University.
§ College of North Atlantic.
|| Department of Biochemistry, University of Western Ontario.
⊥ National Institute for Nanotechnology.

10.1021/jp711925b CCC: $40.75
Published on Web 03/12/2008

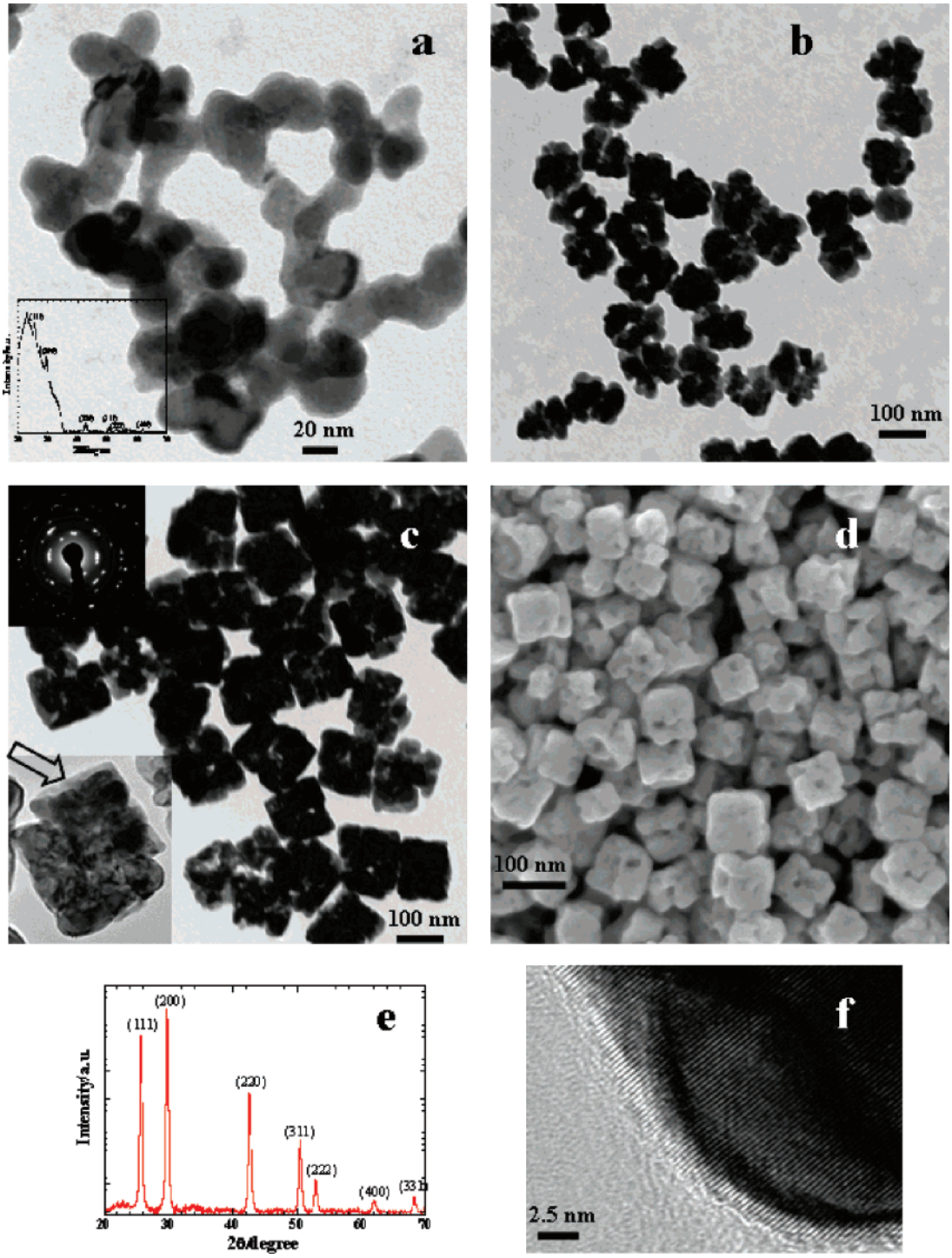

Figure 1. Panel a shows the TEM image of polyhedral PbS nanoparticles synthesized in the presence of [PSS] = 0.5 mM that are arranged in a typical pearl-necklace model due to the amorphous nature indicated by the XRD patterns (inset). Panel b shows the TEM image of PbS NCs with serrated margins synthesized in the presence of [PSS] = 1 mM. Each NC shows the presence of at least one hole. Panel c shows the TEM image of roughly cubic PbS NCs with serrated margins synthesized in the presence of [PSS] = 2 mM. A diffraction image (upper left, inset) shows the polycrystalline nature, and a high-resolution image of a single NC (lower left, inset) shows a thin film of PSS indicated by a block arrow. Panel d shows a FESEM image of panel c. Panel e shows XRD diffraction patterns of panel c. (f) HRTEM image showing crystal planes of panel c.

washings with methanol. Similar reactions were performed at 1, 2, and 4 mM solutions of both PSS and PVP to observe the effect of polymer concentration on the shape and size of PbS NCs.

Methods. The shape and size of PbS NCs were characterized by transmission electron microscopy (TEM). The samples were prepared by mounting a drop of a solution on a carbon coated Cu grid and allowing it to dry in air. The samples were observed with the help of a Philips CM10 transmission electron microscope operating at 100 kV. The high-resolution TEM (HRTEM) and high-angle annular dark field (HAADF) scanning TEM were carried out with the help of CM20. A Hitachi S-4800 field emission scanning electron microscopy (FESEM) instrument was used for all SEM studies. Each sample was diluted with deionized water, then coated with a 4 nm Cr film (Gatan PECS 682 ion beam sputtering). The accelerating voltage was 5 kV.

The X-ray diffraction (XRD) patterns were characterized by using a Bruker-AXS D8-GADDS instrument with $T_{second} = 480$.

Results and Discussion

Figure 1a shows the PbS NCs synthesized in the presence of [PSS] = 0.5 mM. Fused nanoparticles (31.9 ± 8.4 nm) (size histogram is shown in the Supporting Information, Figure S1) in a typical pearl-necklace model without any clear boundaries were obtained. XRD (see inset in Figure 1a) patterns of this sample indicate the amorphous nature of the nanoparticles. An insufficient amount of capping material generally led to the amorphous nature.[2h] At 1 mM (Figure 1b), NCs (108 ± 23.6 nm, Figure S2) with serrated boundaries began to break away. As the concentration increased further (i.e., 2 mM (Figure 1c)), polycrystalline (see inset, upper left of Figure 1c) cubic-shaped NCs (140 ± 28 nm, Figure S3) began to emerge with clear holes. A magnified view of a single NC (see inset, lower left corner of Figure 1c) indicates that such a geometry emerged from the fusion of small polyhedral NPs. During the course of such a fusion, some empty spaces were left in the form of holes. This image also indicates the presence of a thin transparent film on the surface of cubic NCs (shown by a block arrow). The corresponding FESEM image (Figure 1d) further clarifies the topography of each NC. Although the overall shape is roughly cubic, the sides of the cube are rather marked with pits and holes. XRD (Figure 1e) patterns indicate a predominant growth at the {100} crystal plane of fcc geometry. A HRTEM image (Figure 1f) clearly identifies the {100} planes with a lattice spacing of ≈3 Å.[2a] Apart from this, the competing growth at {111} planes are further evident from a continuous increase in the size from 31.9 to 140 nm with an increase in the amount of PSS from 0.5 to 2 mM. As we move on to even larger amounts of [PSS] = 4 mM, apart from roughly cubic NPs of almost the same size, long cylindrical threads (with a diameter of 141 ± 5 nm and length of several micrometers) along with fibrous sheets of such threads were obtained (Figure 2a,b). Figure 2c shows a magnified image of a single thread that is crystalline in nature. Each thread is a single crystal (see diffraction image, inset, upper right of Figure 2c) and is also covered by a thin 3−5 nm PSS film. The HAADF image (inset, lower left of Figure 2c) identifies the film from the crystalline thread due to a difference in the nature of the surface patterns. EDX analysis[2e,9] (Figure 1d) confirms the presence of Pb and S along with C and O; the latter elements might be due to the presence of polyanions of PSS. XRD patterns (Figure 2e) again suggest a predominant growth at the {100} crystal planes of fcc geometry,[2a] which are even clearly visible from the HRTEM image in Figure 1f.

The use of PVP as a capping agent shows the formation of cubic geometries[2c] but without any nanothreads. At [PVP] = 0.5 mM (Figure 3), mostly star-shaped micrometer-sized microcrystals were obtained. As the amount of PVP increased to 1 mM (Figure 1b), the amount of star-shaped microcrystals decreased, and cubic geometries (495 ± 170 nm, Figure S4) appeared. A further increase in concentration of PVP to 4 mM (Figure 1c) led to a complete elimination of the star-shaped microcrystals and produced only fine PbS nanocubes (148 ± 11.6 nm, Figure S5) (75%) with few nanobars (aspect ratio was 2.2 ± 0.05) (25%). A combination of such morphologies is clearly evident from the FESEM images (Figure 3d). Apart from this, one can clearly observe the presence of capping PVP films around each NC as indicated by block arrows in Figure 3c,d. Coresponding XRD (Figure 3e) patterns confirm a much prominent growth at the {100} planes, and this growth might lead to nanobar formation.

All results shown in Figures 1−3 suggest that although both PSS and PVP are water soluble polymers, there seems to be a significant difference among their capping abilities due to the polyelectrolytic and neutral nature of PSS and PVP, respectively. In the case of semiconductor materials such as PbS, the {111} planes of fcc geometry occupy a greater atomic density than the {100} planes. PSS, although not a surfactant, would certainly prefer to adsorb at the {111} crystal planes electrostatically[2c,10] due to its polyanionic property and thereby direct further crystal growth at the {100} planes. However, the insufficient amount of PSS (0.5 mM) cannot control the crystal growth; thus, amorphous NPs[1h,11] arrange in a pearl-necklace arrangement due to cohesive interactions (Figure 1a). An increase in the amount of PSS engulfed the small nucleating centers and promoted crystal growth at the {100} facets, thus preventing amorphous NP formation. Predominant crystal growth at the {100} planes is in fact responsible for the appearance of cubic geometries. A perfect cubic geometry has never been achieved because simultaneous less predominant growth at the {111} planes also takes place (Figure 1e). On the other hand, the formation of nanothreads and nanosheets (Figure 2a,b) at higher PSS concentrations might be due to the soft template effect of some self-assembled states of PSS[12] generated in the presence of lead acetate (i.e., due to ionic effects). Although it is not clear especially as to what kind of self-assembled state facilitates the formation of nanothreads and nanosheets; however, recent studies have demonstrated that polyelectrolyte and mesoporous silica based films are the best templates for organized assemblies of PbS.[6,2c,f,13] In the present work, since all reactions were carried out under static conditions, the formation of polyelectrolyte films at the liquid/solid interface cannot be completely ruled out. Apart from this, recently, Wang and Yang[14] reported the synthesis of PbS nanorods in poly(vinyl butyral) films and PbS nanoparticles in solution. They demonstrated that nanorods were bound with {100} crystal planes obtained in the polymer films due to their lamellar structures, while NP formation takes place only in solution. We believe that [PSS] = 4 mM also may lead to the formation of such self-assembled layered structures that may act as soft templates to produce nanothreads and nanosheets. The soft template effect of PSS is considered to be the most likely reason for the 1-D nanostructure formation because no shape transformation from roughly cubic geometries to nanothreads has been observed from TEM analysis with respect to an increase in the amount of PSS.

Like conventional surfactants, PVP also is expected to predominantly adsorb at the {111} planes due to electrostatic interactions, which originate from the lone pair of oxygen atoms on the carbonyl group of the pyrrolidone moiety. Thus, PVP also directs the crystal growth at the {100} crystal planes just like that of PSS. One can very well understand this phenomenon from the smooth transition of star-shaped geometries into perfect cubic nanocrystals as the amount of PVP increases. A perfect cubic geometry bound with {100} planes suggests a complete coverage of {111} crystal planes by PVP molecules. Although PSS should have an even much stronger adsorption at the {111} facets due to its polyanionic nature, the presence of roughly cubic geometries indicates a somewhat different mechanism, where competing growth at the {111} and {100} facets is observed (Figure 1e). This means that PSS not only has preferential surface adsorption for {111} crystal planes but it has some tendency to adsorb at even the {100} planes due to its polyanionic nature. Otherwise, a clear cubic geometry might have emerged from each polyhedral amorphous nanoparticle

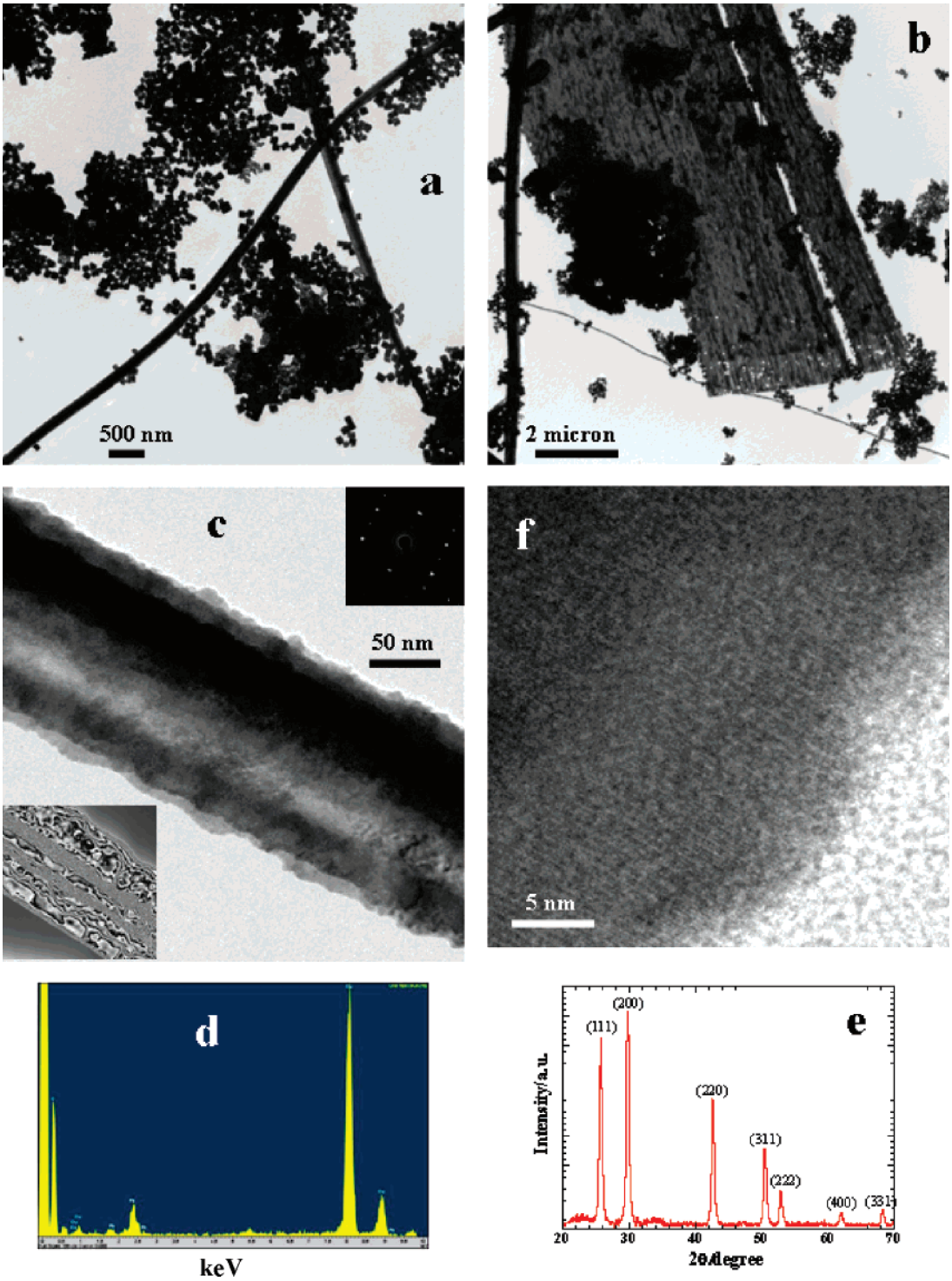

Figure 2. Panel a shows the TEM image of roughly cubic PbS NCs along with PbS nanothreads of several micrometers in length synthesized in the presence of [PSS] = 4 mM. Panel b shows the presence of threads in the form of nanosheets along with the roughly cubic PbS NCs of the same sample. Panel c shows a section of a single thread coated with a thin film of PSS. A diffraction image (upper right, inset) shows the crystalline nature, and a HAADF image (lower left, inset) shows the surface pattern due to the presence of the PSS film. (d) EDX spectrum showing the surface analysis of single threads. (e) XRD patterns of panel a. (f) HRTEM image showing crystal planes of single threads of panel c.

just like that in the presence of PVP (Figure 3c). Such a capping behavior of PSS, where PSS specifically controls the shape evolution from amorphous to crystalline NCs, is quite unique, and this article seems to be the first report in literature as far as our information is concerned. This is further evident from the intensity ratio difference (I_{100}/I_{111}) for PbS NC formation in 4 mM PSS and PVP. This ratio is much smaller for PSS (1.1) than PVP (1.5), suggesting a competing growth at both planes in the former case, while there is preferential growth only at the {100} planes[12a] in the latter case, and that governs the overall growth in each case. On the other hand, PSS demonstrates a soft template effect with the result of which nanothreads and nanosheets are formed. But, the latter geomeries are altogether absent at 4 mM PVP, probably due to the absence of any soft template effect. Therefore, within the concentration range studied herein, it can be said that PSS produces better templating effects for PbS 1-D nanostructures, while PVP, on the other hand, proves to be a better shape directing agent.

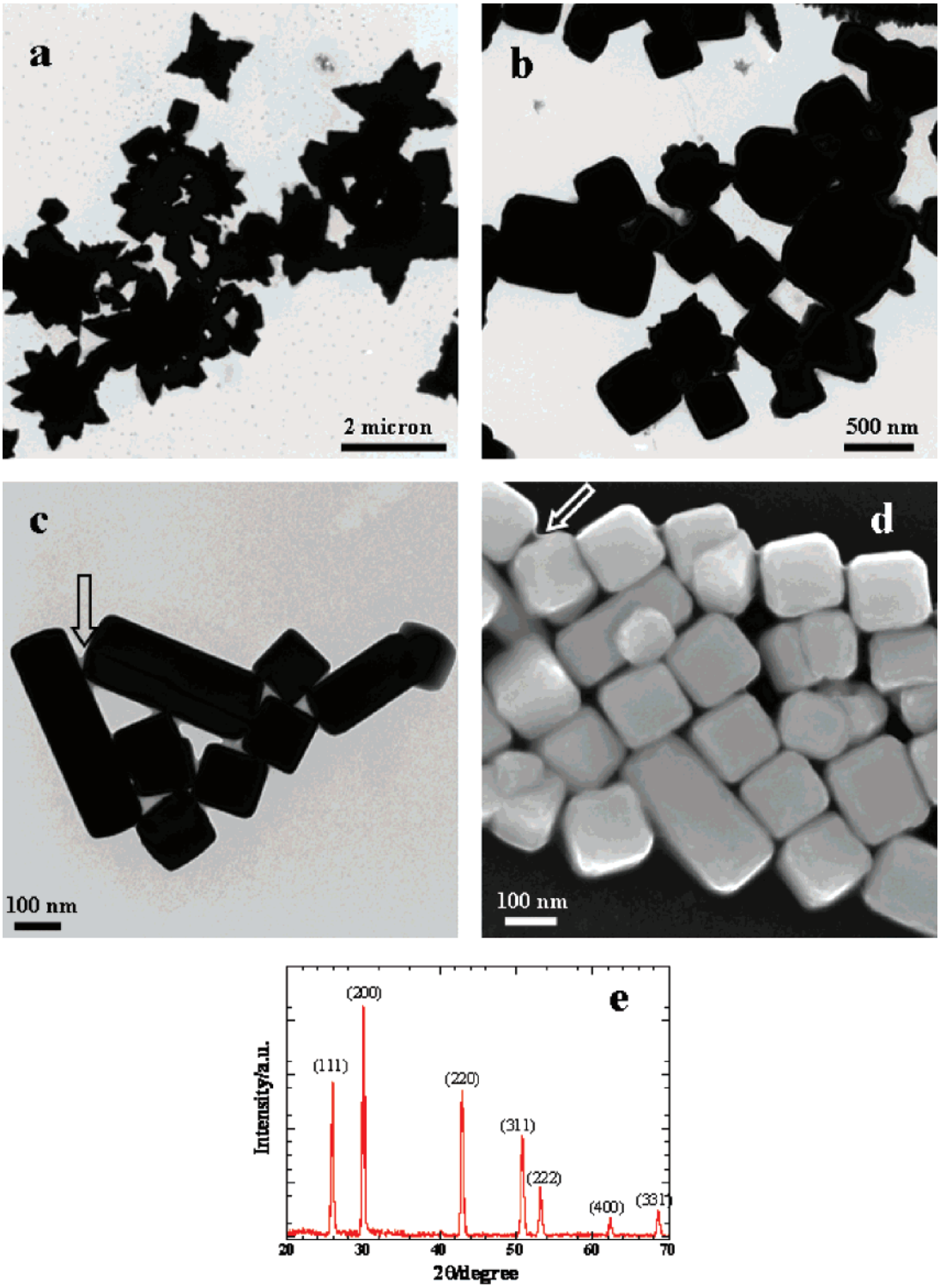

Figure 3. Panel a shows the TEM image of star-shaped PbS NCs in the presence of [PVP] = 0.5 mM. Panel b shows the TEM image of mostly cubic geometries of PbS NCs in the presence of [PVP] = 1 mM. Panel c shows the TEM image of fine cubic NCs and nanobars of PbS in the presence of [PVP] = 4 mM. A block arrow indicates the presence of the PVP capping film. Panels d and e show the FESEM image and XRD patterns, respectively, of the same sample.

Conclusion

These results conclude that the capping ability of a water soluble polymer (i.e., PSS and PVP) significantly controls the crystal growth of PbS NCs. PSS has a strong affinity to interact electrostatically at different crystal planes, while PVP preferentially adsorbs at {111} crystal planes and thus produces perfect cubic geometries bonded with {100} planes. PSS mostly produces polycrystalline roughly cubic NCs with competing growth at the {111} as well as {100} crystal planes at low concentrations. At high concentrations, 1-D nanostructures, such as nanothreads and nanosheets, are produced due to the soft template effect of self-assembled PSS films.

Acknowledgment. This study was supported by Grants MOP 66406 and FRN 15462 from the Canadian Institutes of Health Research.

Supporting Information Available: Structures of PSS and PVP and size histograms. This material is available free of charge via the Internet at http://pubs.acs.org.

References and Notes

(1) Jun, Y.-W.; Choi, J.-S.; Cheon, J. *Angew. Chem., Int. Ed*. **2006**, *45*, 3414.

(2) (a) Patla, I.; Acharya, S.; Zeiri, L.; Israelachvili, J.; Efrima, S.; Golan, Y. *Nano Lett.* **2007**, *7*, 1459. (b) Talapin, D. V.; Yu, H.; Shevchenko, E. V.; Lobo, A.; Murray, C. B. *J. Phys. Chem. C* **2007**, *111*, 14049. (c) Zhou, G.; Lü, M.; Xiu, Z.; Wang, S.; Zhang, H.; Zhou, Y.; Wang, S. *J. Phys. Chem. B* **2006**, *110*, 6543. (d) Zhou, Y.; Itoh, H.; Uemura, T.; Naka, K.; Chujo, Y. *Langmuir* **2002**, *18*, 5287. (e) Gao, F.; Lu, Q.; Liu, X.; Yan, Y.; Zhao, D. *Nano Lett.* **2001**, *1*, 743. (f) Wang, S. F.; Gu, F.; Lü, M. K. *Langmuir* **2006**, *22*, 398. (g) Ma, Y.; Qi, L.; Ma, J.; Cheng, H. *Cryst. Growth Des.* **2004**, *4*, 351. (h) Bakshi, M. S.; Thakur, P.; Sachar, S.; Kaur, G.; Banipal, T. S.; Possmayer, F.; Petersen, N. O. *J. Phys. Chem. C* **2007**, *111*, 18087.

(3) (a) Patolsky, F.; Zheng, G.; Hayden, O.; Lakadamyali, M.; Zhuang, X.; Lieber, C. M. *Proc. Natl. Acad. Sci. U.S.A.* **2004**, *101*, 14017. (b) Law, M.; Greene, L. E.; Johnson, J. C.; Saykally, R.; Yang, P. *Nat. Mater.* **2005**, *4*, 455. (c) Hayden, O.; Agarwal, R.; Lieber, C. M. *Nat. Mater.* **2006**, *5*, 352.

(4) Joly, S.; Kane, R.; Radzilowski, L.; Wang, T.; Wu, A.; Cohen, R. E.; Thomas, E. L.; Rubner, M. F. *Langmuir* **2000**, *16*, 1354.

(5) Cho, K.-S.; Talapin, D. V.; Gaschler, W.; Murray, C. B. *J. Am. Chem. Soc*. **2005**, *127*, 7140.

(6) (a) Schuetz, P.; Caruso, F. *Chem. Mater*. **2004**, *16*, 3066. (b) Yang, H.; Holloway, P. H. *J. Phys. Chem. B* **2003**, *107*, 9705.

(7) Roucoux, A.; Schulz, J.; Patin, H. *Chem. Rev.* **2002**, *102*, 3757.

(8) (a) Bai, J.; Qin, Y.; Jiang, C.; Qi, L. *Chem. Mater.* **2007**, *19*, 3367. (b) Wiley, B. J.; Chen, Y.; McLellan, J. M.; Xiong, Y.; Li, Z.-Y.; Ginger, D.; Xia, Y. *Nano Lett.* **2007**, *7*, 1032. (c) Wang, Y.; Li, Y.; Yang, S.; Zhang, G.; An, D.; Wang, C.; Yang, Q.; Chen, X.; Jing, X.; Wei, Y. *Nanotechnology* **2006**, *17*, 3304. (d) Gao, Y.; Jiang, P.; Liu, D. F.; Yuan, H. J.; Yan, X. Q.; Zhou, Z. P.; Wang, J. X.; Song, L.; Liu, L. F.; Zhou, W. Y.; Wang, G.; Wang, C. Y.; Xie, S. S. *J. Phys. Chem. B* **2004**, *108*, 12877. (e) Zhang, D.; Qi, L.; Yang, J.; Ma, J.; Cheng, H.; Huang, L. *Chem. Mater*. **2004**, *16*, 872.

(9) Warner, J. H.; Watt, A. A. R. *Mater. Lett.* **2006**, *60*, 2375.

(10) Zhao, N.; Qi, L. *Adv. Mater.* **2006**, *18*. 359.

(11) (a) Lemyre, J.-L.; Ritcey, A. M. *Chem. Mater.* **2005**, *17*, 3040. (b) Cöffen, H.; Xu, A.-W.; Dong, W. *Cryst. Growth Des.* **2004**, *4*, 33.

(12) (a) Katchalasky, A.; Zwick, M. *J. Polym. Sci.* **1955**, *16*, 221. (b) Zezin, A. B.; Rogacheva, V. B.; Kabanov, V. A. *Macromol. Symp.* **1997**, *126*, 123.

(13) (a) Wang, S.; Yang, S. *Langmuir* **2000**, *16*, 389. (b) Patel, A. A.; Wu, F.; Zhang, J. Z.; Torres-Martinez, C. L.; Mehra, R. K.; Yang, Y.;. Risbud, S. H. *J. Phys. Chem. B* **2000**, *104*, 11598.

(14) Wang, S.; Yang, S. *Langmuir* **2000**, *16*, 389.